Direct-Write Piezoelectric Polymeric Nanogenerator with High Energy Conversion Efficiency

Chieh Chang,[*,†] *Van H. Tran,*[†,‡] *Junbo Wang,*[†,§] *Yiin-Kuen Fuh,*[†] *and Liwei Lin*[†]

Berkeley Sensor and Actuator Center, Department of Mechanical Engineering, University of California, Berkeley, CA 94720, USA

* To whom correspondence should be addressed. E-mail: chieh@berkeley.edu

RECEIVED DATE (to be automatically inserted after your manuscript is accepted if required according to the journal that you are submitting your paper to)

† Berkeley Sensor and Actuator Center, Department of Mechanical Engineering, University of California, Berkeley, CA 94720, USA

‡ Department of Medical Engineering, Faculty of Mechanical Engineering, Technische Universität München, Germany

§ State Key Laboratory of Transducer Technology, Institute of Electronics, Chinese Academy of Sciences, Beijing, China

ABSTRACT

Nanogenerators capable of converting energy from mechanical sources to electricity with high effective efficiency using low-cost, non-semiconducting, organic nanomaterials are attractive for many applications, including energy harvesters. In this work, near-field electrospinning is used to direct-write polyvinylidene fluoride (PVDF) nanofibers with in-situ mechanical stretch and electrical poling

characteristics to produce piezoelectric properties. Under mechanical stretching, nanogenerators have shown repeatable and consistent electrical outputs with energy conversion efficiency an order of magnitude higher than those made of PVDF thin films. The early onset of the nonlinear domain wall motions behavior has been identified as one mechanism responsible for the apparent high piezoelectricity in nanofibers, rendering them potentially advantageous for sensing and actuation applications.

MANUSCRIPT TEXT

Mechanical energy scavenging from ambient environments is an attractive renewable source of power for various applications. Examples range from large-scale power generators which convert mechanical actuation found in nature, such as waterfalls, wind, and ocean waves, into electricity[1,2] to small-scale energy harvesters which scavenge energy from mechanical vibration sources in building, automotives, appliances, and human movements[3,4]. In pursuing these mechanical energy harvesters, especially for small-scale applications, one fundamental issue is the design and selection of structural materials for efficient conversion of mechanical energy into electricity. Recent work in the field of nanomaterials has provided new opportunities and directions in engineering effective materials and structures for energy harvesters. Prior research[5–8] on energy scavenging using zinc oxide (ZnO) nanowires has illustrated the feasibility of utilizing inorganic nanomaterials with semiconducting and piezoelectric properties for nanogenerators. Further advancements for nanogenerators include the utilization of non-semiconducting and organic nanomaterials, direct-integration with other structures and processes, and improvements in energy conversion efficiency. Here, we report direct-write, piezoelectric polymeric nanogenerators based on organic nanofibers with high energy conversion efficiency to address some of the aforementioned challenges. These nanofibers are made of polyvinylidene fluoride (PVDF) with high flexibility, minimizing resistance to external mechanical movements in low-frequency, large-deflection energy scavenging applications. PVDF has good piezoelectric and mechanical properties, exhibits chemical stability and weathering characteristics[9–11], and is usually constructed as thin films for sensing and actuation applications[12–15]. However, untreated PVDF can have α, β and γ crystalline

phases and must be mechanically stretched and electrically poled to obtain the β phase necessary for generating piezoelectricity[16, 17].

We utilize a direct-write technique by means of near-field electrospinning (NFES)[18, 19] to produce and place piezoelectric PVDF nanofibers on working substrates with *in-situ* mechanical stretching and electrical poling (Figure 1a). The strong electric fields (greater than 10^7 V/m) and stretching forces from the electrospinning process naturally align dipoles in the nanofiber crystal such that the non-polar α phase (random orientation of dipoles) is transformed into polar β phase, determining the polarity of the electrospun nanofiber. The as-spun PVDF nanofibers have diameters ranging from 500 nm to 6.5 μm with variable lengths defined by the separation distance (100 – 600 μm) between two metallic electrodes (Figure 1b). When an axial stress is applied by bending the plastic deposition substrate, a piezoelectric potential is generated. The piezoelectric constant, g_{33}, of PVDF is negative such that stretching PVDF nanofibers along the poling axis generates a voltage with the polarity opposite to the electric field direction (the poling axis) during the electrospinning process. Therefore, a positive voltage output is expected by connecting the positive port of the multimeter to the distal end of the electrospun nanofiber. When the substrate is stretched and released repeatedly, voltage and current outputs can be recorded, respectively (Figure 1c, d). The typical electrical outputs of more than 50 tested nanogenerators were 5 – 30 mV and 0.5 – 3 nA. Experiments of both non-piezoelectric polyethylene oxide nanofibers and randomly distributed PVDF nanofibers fabricated by the conventional electrospinning process show no measureable electrical outputs, mainly noise which rules out the possibility of artifacts (Figure S1 and S2, Supplementary Information).

As the strain is released from the nanogenerator, corresponding negative peaks can be observed in both the output voltage and current measurements. This phenomenon can be explained by examining the equivalent circuit model of the nanogenerator in Figure 2a. The PVDF nanogenerator is modeled as a charge source in parallel with a capacitor C_G and a resistor R_G with estimated values of 160 pF and 15 GΩ, respectively (Figure 2b). Mechanical strain can induce piezoelectric bound charges (polarization) which results in a potential difference at the two ends of the nanogenerator. Since the nanogenerator

has a large internal resistance, there is little charge leakage/loss in the nanogenerator during the short period of the stretch-hold-release experiments (Figure 2c). During the stretch process, the piezoelectric bound charges induced a built-in potential in the nanogenerator. In response, the external free charges (yellow line in Figure 2c) are driven to the nanogenerator to neutralize this potential at a speed set by both the external circuitry and the built-in potential. During this process, the net charge (red line in Figure 2c) increases with the piezoelectric bound charges at a rate that is faster than the flow of the external free charges. At a constant strain (the strain is on hold), both the net charges and the built-in potential gradually diminish to zero as the piezoelectric bound charges are balanced by the free charges. When the strain is released, the piezoelectric potential diminishes and the free charges that have accumulated at both ends of the nanofiber generate an opposing potential. The free charges gradually flow back in a direction opposite to the accumulation process and the current reduces to zero (green line in Figure 2c) at a rate set by the external circuitry.

The electrical outputs are also affected by the strain rate. For a strain of 0.085% applied over 0.04 and 0.10 seconds, output currents of 2.74 and 1.16 nA were experimentally measured , respectively, with charges similar in both experiments (Figure 3a). Specifically, the small discrepancy in piezoelectric charges between186 pC for fast strain rate experiments and 175 pC for slow strain rate experiments results from the *RC* time constant of the nanogenerator (*c*. 2.4 second) which allows a small portion of piezoelectric charge to leak through. In the fast strain rate (*c*. 0.17 second) and slow strain rate (*c*. 0.33 second) experiments, there are estimated *c*. 6.8% and *c*. 12.8% of the piezoelectric charges leaking through the nanogenerator, respectively. This corresponds to *c*. 93.2% and *c*. 87.2% of the piezoelectric charges that are neutralized by the free charges through the external circuitry, from the same peak value of *c*. 200 pC in both cases. The results are consistent with fundamental piezoelectric theory $i = \dot{q} = d_{33} EA\dot{\varepsilon}$ [20], where i is the generated current, q is the generated charge, d_{33} is the piezoelectric charge constant, E is the Young's modulus, A is the cross-sectional area, and $\dot{\varepsilon}$ is the applied strain rate.

Figure 3b, c show the responses of the nanogenerator under various cycling frequencies ranging from 2 to 4 Hz for the same applied external strain. The output voltage and current during the stretch cycle increase with the frequency, while they remain approximately constant during the release cycle; a phenomenon that can be attributed to the applied strain rate. In the experimental setup, the loading machine controls the stretching profile and therefore the increases in both the strain rate and cycling frequency for a given applied strain. The release process is the release of the cantilever beam substrate from the strained position, which restores the nanogenerator to its original state. The speed with which it reaches this state is controlled by the substrate rigidity, resulting in a higher strain rate that dominates electrical outputs more than the cycling frequency. It is also noted that the output impedance of the nanogenerator varies with frequency and as the cycling frequency increases from 2 to 4 Hz, the impedance drops from 900 MΩ to 300 MΩ (Figure 2b). This leads to better impedance matching with the measurement system and results in higher electrical outputs. The long-term stability of the PVDF piezoelectric nanogenerator is examined through operation over an extended period of time and exposing it to the ambient environment sans protective packaging. For these experiments, the electrical outputs were relatively stable without noticeable degradation for a stretch-release cycle frequency of 0.5 Hz and an operation time of 100 minutes (Figure 4). It was also found that the output voltage and current of the PVDF nanogenerator could be enhanced by serial and parallel connections, respectively (Figure S3). The electrical outputs of serial and parallel connections are approximately the sum of the two individual nanogenerators, which satisfies the "linear superposition" criterion proposed by Yang *et al* [8] to confirm the true piezoelectric responses. This is achieved by the direct-write characteristics of NFES, as the placement and polarity of the PVDF nanofibers can be manipulated such that nanofibers are in either serial or parallel connections during the fabrication process.

The energy conversion efficiency of the PVDF nanogenerator can be estimated as the ratio between generated electrical energy and applied mechanical energy. The output electrical energy generated by stretching the piezoelectric nanofiber is calculated as: $W_e = \int VIdt$, where V and I are the measured output voltage and current, respectively. The total elastic strain energy stored in the nanofiber is

approximated as: $W_s = \frac{1}{8}\pi D^2 E \varepsilon^2 L_0$ [8], where D is diameter of the nanofiber, L_0 is the length of the nanofiber, E is the Young's modulus, and ε is the strain applied on the nanofiber. The efficiency of converting mechanical energy to electrical energy is given by the ratio W_e/W_s. By analyzing 45 samples, the energy conversion efficiency of our nanogenerators was found to be as high as 21.8% with an average of 12.5%, a value that is much greater than typical power generators made from experimental piezoelectric PVDF thin films (0.5 – 4%)[21–24] and commercial PVDF thin films (0.5 – 2.6%) tested under the same conditions in this work (Figure 5a and Supplementary Information). Furthermore, the general trend indicates that nanogenerators with smaller diameters exhibit higher energy conversion efficiencies, even with variable piezoelectric properties resulting from slight changes in processing conditions. Several possible reasons could have contributed to the observed enhanced electromechanical response. For example, previous reports have demonstrated a drop in the piezoelectric coefficient due to internal defects in ultrathin PZT films[25], while nanogenerators made by the NFES process could possibly have fewer defects than the PVDF thin film due to a higher degree of crystallinity and chain orientation[26]. The difference in elastic boundary conditions (thin film/bulk samples have metal electrodes on both ends as constraints)[27] and the physical size of the nanogenerators could promote size dependent piezoelectricity such as "flexoelectricity", which is caused by strain gradients that locally break inversion symmetry and induce polarization[28]. Furthermore, piezoelectric thin films could have a significant fraction of the measured responses coming from extrinsic contributions collectively known as "domain wall motion"[29]. PVDF thin film material has a domain wall motion barrier at *c*.0.3% strain[30], under which the piezoelectric response results from the mostly linear, intrinsic response (the responses of single domains). Once the applied strain increases beyond the barrier, the piezoelectric response is dominated by the remarkably large, nonlinear extrinsic responses due to domain wall motion[30]. We observed a much smaller domain wall motion barrier in PVDF nanofibers (*c*.0.01%) as shown in Figure 5b which results in large piezoelectric responses for strain higher than 0.01%. This could be caused by small concentrations of point and line defects in the

nanofibers which improve the contribution of domain wall motion and lead to higher energy conversion efficiency.

In summary, we have demonstrated PVDF nanogenerators that are directly written onto flexible plastic substrate using NFES. The piezoelectric responses of single PVDF nanofibers were measured and multiple nanofibers were arranged to enhance the electrical outputs. The reported nanogenerator has several advantages over other maco-, micro-, and nanogenerators, including high energy conversion efficiency, manufacturability, and the capability of integration with other micro/nanofabrication processes. The principle and the nanogenerator demonstrated could be the basis for integrated power source in nanodevices and wireless sensors or new self-powered textile by direct-writing nanofibers onto a large area cloth to boost the total power output for portable electronics.

SUPPORTING INFORMATION

Materials, methods, validation of piezoelectric responses, and more details on energy conversion efficiency.

FIGURE CAPTIONS

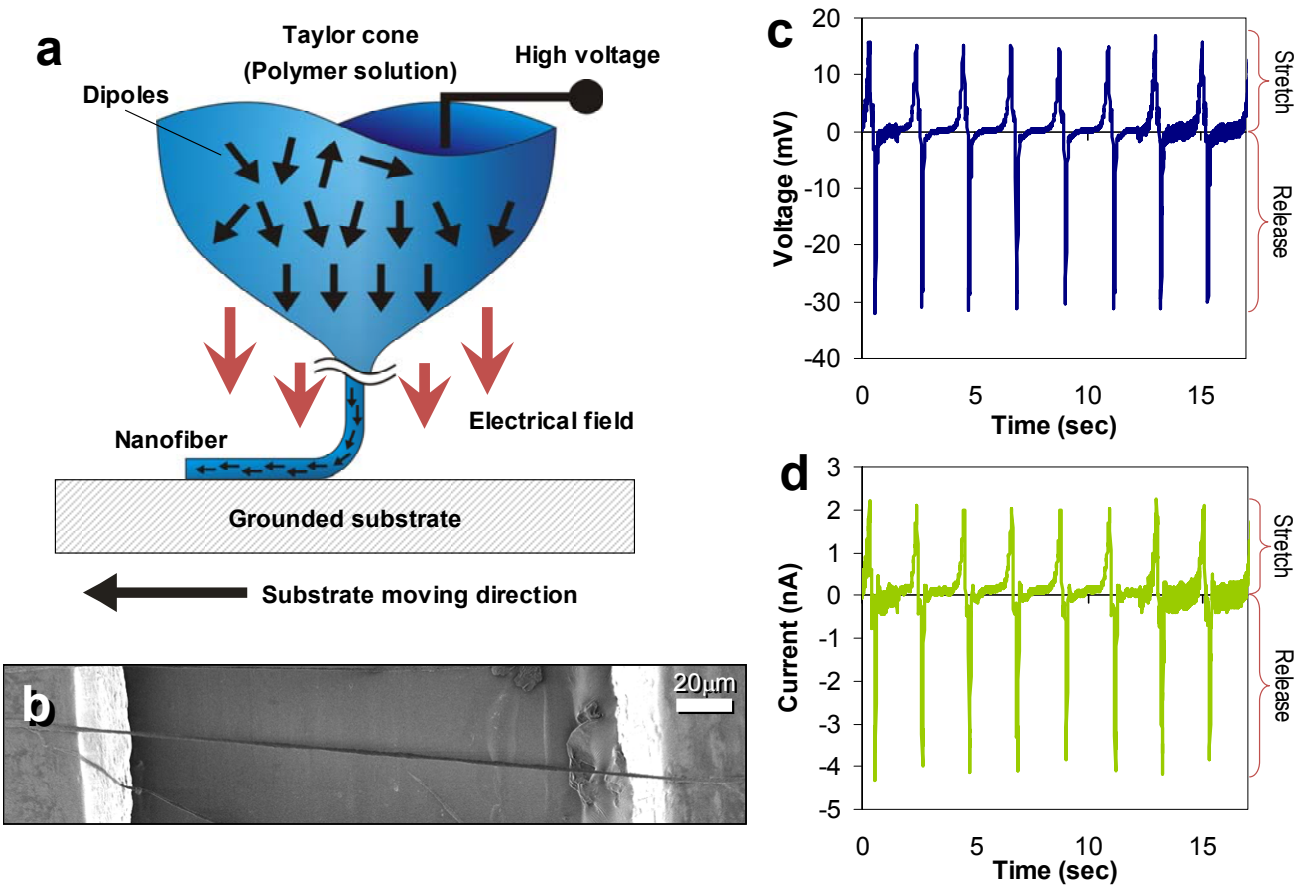

Figure 1. Piezoelectric PVDF nanogenerator. (a) Near-field electrospinning (NFES) combining direct-write, mechanical stretching, and in-situ electrical poling to create and place piezoelectric nanogenerators onto a substrate. (b) Scanning electron microscope (SEM) image of a nanogenerator comprised of a single PVDF nanofiber, two contact electrodes, and a plastic substrate. (c) Output voltage measured with respect to time under an applied strain at 2Hz. (d) Output current measured with respect to time under applied strain at 2Hz.

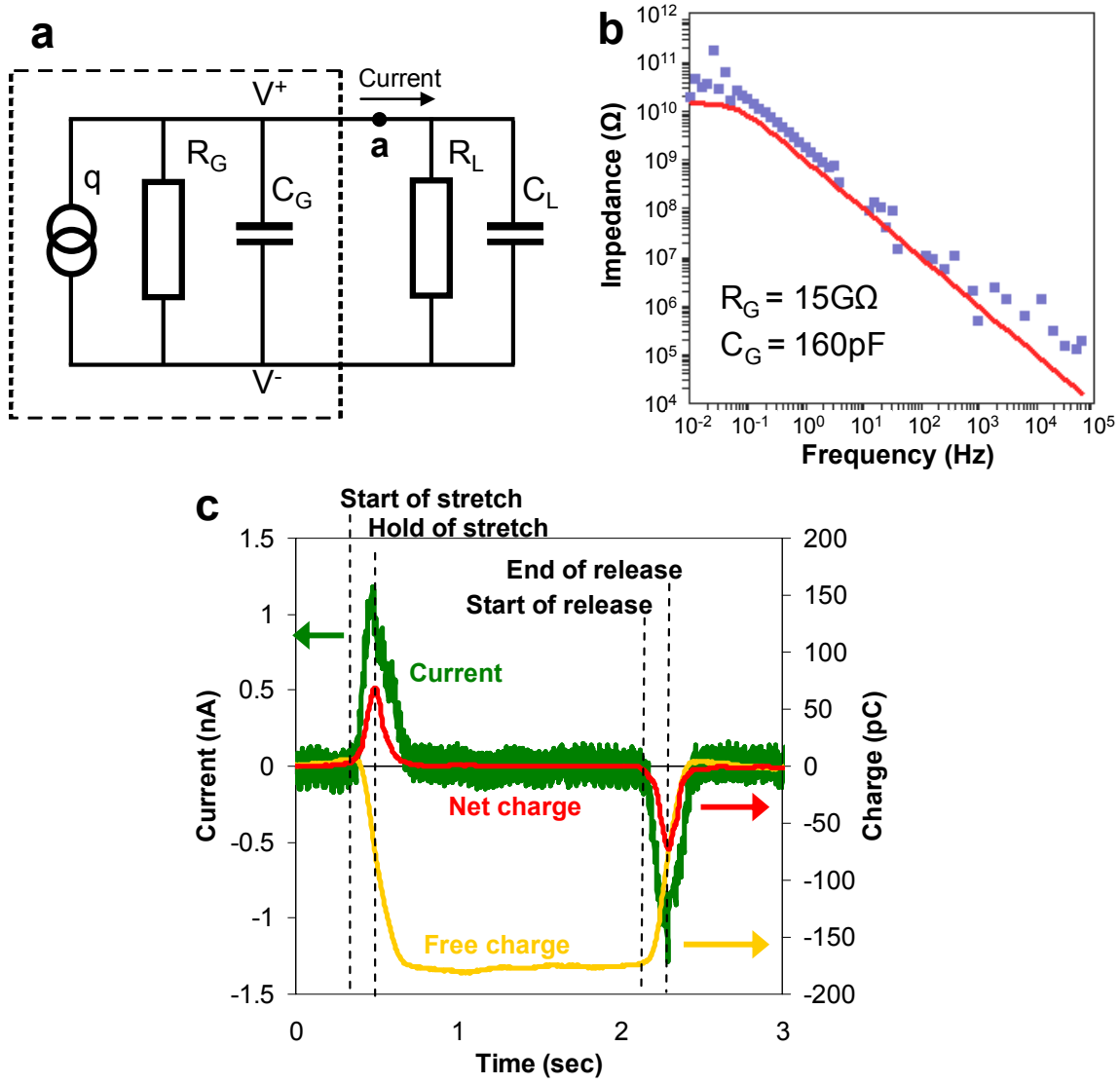

Figure 2. Electric model of a piezoelectric PVDF nanogenerator. (a) The equivalent circuit of a piezoelectric PVDF nanogenerator connected to readout circuit with an equivalent load resistor, R_L and capacitor, C_L. The piezoelectric nanogenerator is modeled as a charge generator q, parallel to a capacitor C_G and a resistor R_G. The positive output current is defined as the current flow from node a (distal end of the electrospun nanofiber) to the readout circuit. (b) Impedance measurement (blue dots) and data-fitted analytical model (red solid line) of the PVDF nanogenerator. (c) Charge movements during the stretch and release of the PVDF nanogenerator. The green line represents the measured output current during the stretch and release stages. The yellow line, which is generated from the integral of measured output current, represents the external free charges (electrons) transported from

external wires to the nanogenerator. The red line represents measured net charges (holes) of the PVDF nanogenerator.

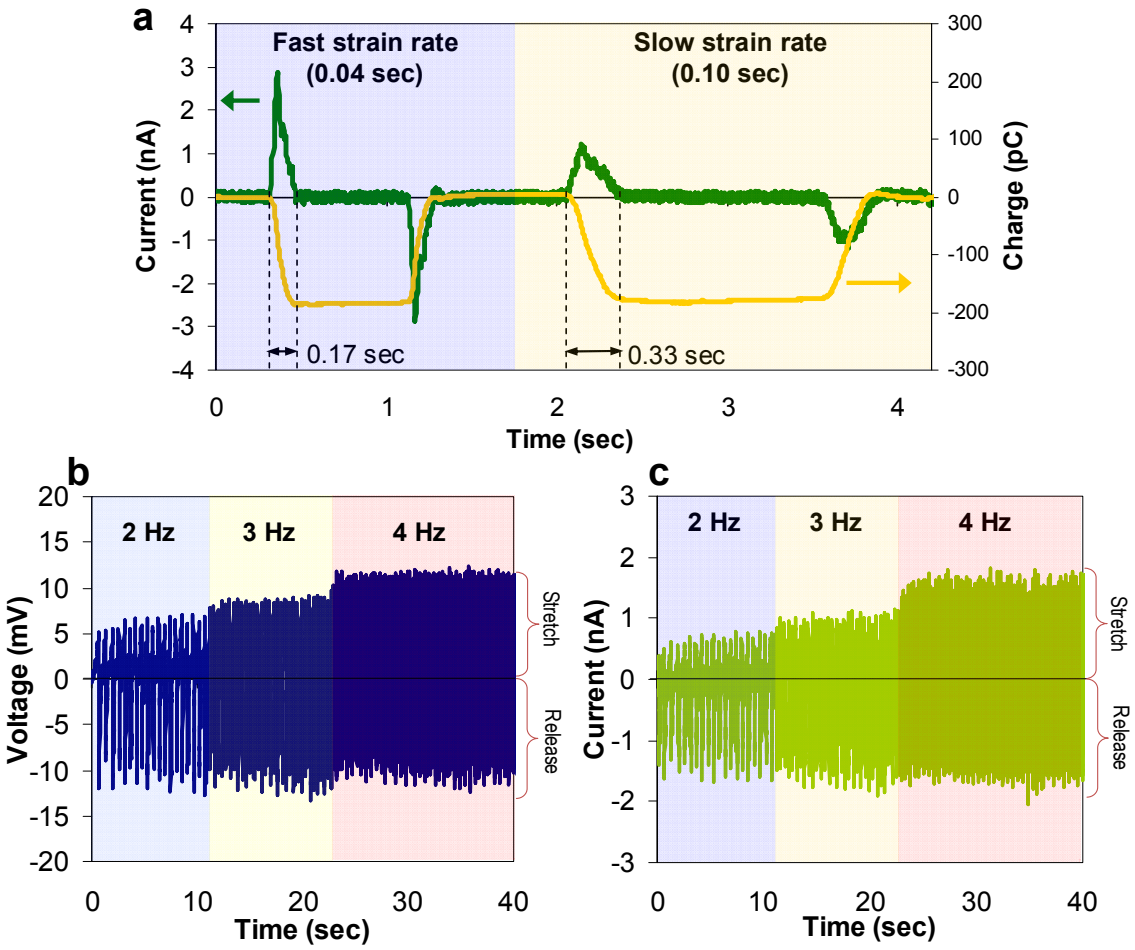

Figure 3. Electric output of a piezoelectric PVDF nanogenerator. (a) Output current (green line) of a PVDF nanogenerator subject to different strain rates under the same applied total strain. The current output increases with strain rate. However, the total charges generated (yellow line, from integral of the output current) are approximately the same under different strain rates. (b) Output voltage and (c) output current of a PVDF nanogenerator subject to different stretch-release cycling frequencies of 2 to 4Hz.

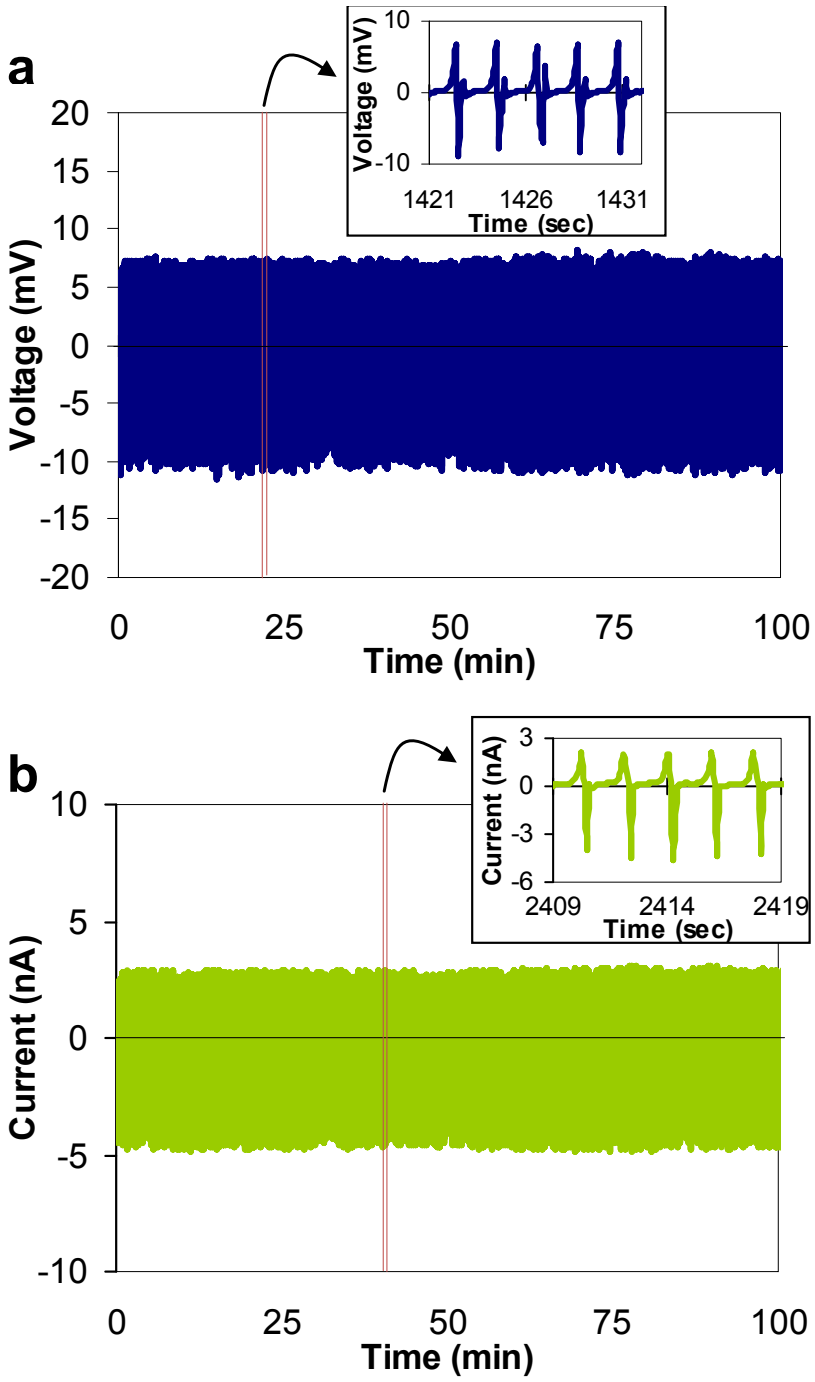

Figure 4. Long term stability tests. (a) Output voltage and (b) output current of a PVDF nanogenerator under 0.5 Hz of continuous stretch-release for 100 minutes, demonstrating the stability of the nanogenerator. The inset shows the detailed profiles of the electrical outputs.

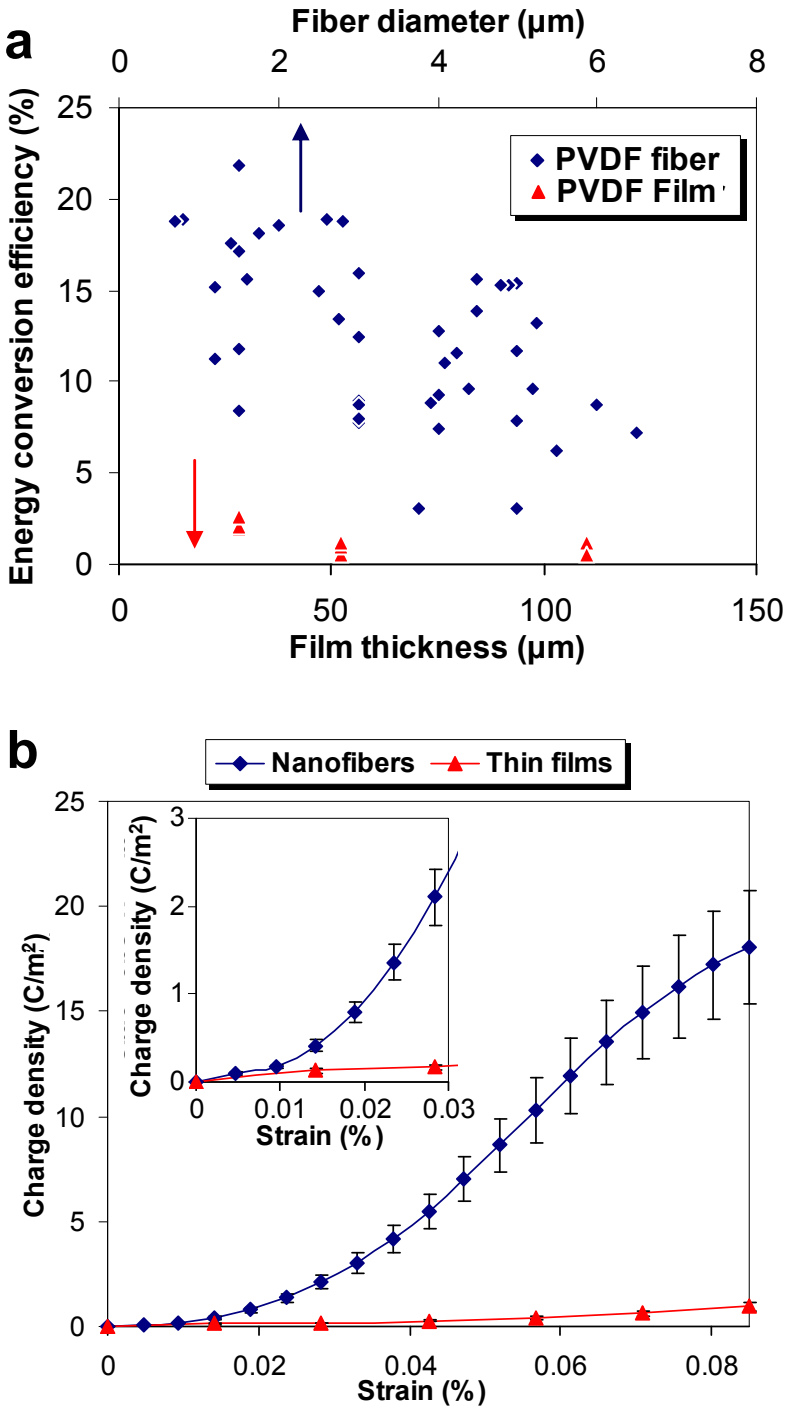

Figure 5. Energy conversion efficiency of a piezoelectric PVDF nanogenerator. (a) Plots of measured energy conversion efficiency of PVDF nanogenerators and thin films with different feature sizes. (b) Experimental results of PVDF thin film and nanofiber charge density (generated charges divided by electrode area) with respect to applied strain. The charge density of PVDF nanofiber increases

nonlinearly when the applied strain is larger than *c.* 0.01%. The inset shows the details under small strains.

REFERENCES

1. Lu, X.; McElroy, M. B.; Kiviluoma, J. Global Potential for Wind-Generated Electricity. *Proc. Natl. Acad. Sci. U.S.A.* **2009**, 106, 10933–10938.
2. Scruggs, J. and Jacob, P. Harvesting Ocean Wave Energy. *Science* **2009**, 323 (5918), 1176-1178.
3. Paradiso, J. A. and Starner, T. Energy Scavenging for Mobile and Wireless Electronics. *IEEE Pervasive Comput.* **2005**, 4 (1), 18–27.
4. Donelan, J. M.; Li, Q.; Naing, V.; Hoffer, J. A.; Weber, D. J.; Kuo, A. D. Biomechanical Energy Harvesting: Generating Electricity During Walking with Minimal User Effort. *Science* **2008**, 319 (5864), 807-810.
5. Wang, Z. L. and Song, J. Piezoelectric Nanogenerators Based on Zinc Oxide Nanowire Arrays. *Science* **2006**, 312 (5771), 242–246.
6. Wang, X.; Song, J.; Liu, J.; Wang, Z. L. Direct-Current Nanogenerator Driven by Ultrasonic. *Science* **2007**, 316 (5821), 102–105.
7. Qin, Y.; Wang, X.; Wang, Z. L. Microfibre-Nanowire Hybrid Structure for Energy Scavenging. *Nature* **2008**, 451, 809–813.
8. Yang, R.; Qin, L.; Dai, L; Wang, Z. L. Power Generation with Laterally Packaged Piezoelectric Fine Wires. *Nat. Nanotech.* **2009**, 4, 34–39.
9. Kawai, H. The Piezoelectricity of Poly(Vinylidene Fluoride). *Jpn. J. Appl. Phys.* **1969**, 8, 975–976.
10. Holmes-Siedle, A.G.; Wilson, P.D.; Verrall, A.P. PVDF: An Electronicallv-Active Polymer for Industry. *Mater. Des.* **1984**, 4, 910–918.
11. Lovinger, A.J. *Dev. Cryst. Polym.* **1982**, 1 (Applied Science Publishers, London).
12. Lee, C. -K. and O'Sullivan, T. C. Piezoelectric Strain Rate Gages. *J. Acoust. Soc. Am.* **1991**, 90, 945–953.
13. Spineanu, A.; Bénabès, P.; Kielbasa, R. A Digital Piezoelectric Accelerometer with Sigma-Delta Servo Technique. *Sens. & Actu. A* **1997**, 60, 127–133.
14. Chen, Z.; Shen, Y.; Xi, N.; Tan, X. Integrated Sensing for Ionic Polymer–Metal Composite

Actuators Using PVDF Thin Films. *Smart Mater. Struct.* **2007**, 16, S262–S271.

15. Lee, Y.-S.; Elliot, S. J.; Gardonio, P. Matched Piezoelectric Double Sensor/Actuator Pairs for Beam Motion Control. *Smart Mater. Struct*. **2003**, 12, 541–548.
16. Calvert, P. Piezoelectric Polyvinylidene Fluoride. *Nature* **1975**, 256, 694.
17. Davis, G. T. Piezoelectric Polymer Transducers. *Adv. Dent. Res.* **1987**, 1, 45–49.
18. Sun, D.; Chang, C.; Li, S.; Lin, L. Near-Field Electrospinning. *Nano Lett.* **2006**, 6 (4), 839–842.
19. Chang, C.; Limkrailassiri, K.; Lin, L. Continuous Near-Field Electrospinning for Large Area Deposition of Orderly Nanofiber Patterns. *Appl. Phys. Lett.* **2008**, 93 (12), 123111-1–123111-3.
20. Sirohi, J. and Chopra, I. Fundamental Understanding of Piezoelectric Strain Sensors. *J. Intell. Mater. Syst. Struct.* **2000**, 11 (4), 246–257.
21. Kymissis, J.; Kendall, C.; Paradiso, J.; Gershenfeld, N. Parasitic Power Harvesting in Shoes. *Second IEEE Int'l Conf. Wearable Computing*, **1998**, 132–139.
22. Häsler, E.; Stein, L.; Harbauer, G. Implantable Physiological Power Supply with PVDF Film. *Ferroelectrics* **1984**, 60 (1), 277–282.
23. Starner, T. Human Powered Wearable Computing. *IBM Syst. J.* **1996**, 35 (3–4), 618–629.
24. Schmidt, V. H. Piezoelectric Energy Conversion in Windmills. *Proc. Ultrasonics Symp.* **1992**, 2 897–904.
25. Dunn, S. Determination of Cross Sectional Variation of Ferroelectric Properties for Thin Film (ca. 500 nm) PZT (30/70) via PFM. *Integr. Ferroelectr.* **2003**, 59 (1), 1505–1512.
26. Gu, S.-Y.; Wu, Q.-L.; Ren, J.; Vancso, G. J. Mechanical Properties of A Single Electrospun Fiber and Its Structures. *Macromol. Rapid Commun.* **2005**, 26 (9), 716–720.
27. Zhao, M.-H.; Wang, Z.-L.; Mao, S. X. Piezoelectric Characterization of Individual Zinc Oxide Nanobelt Probed by Piezoresponse Force Microscope. *Nano Lett.* **2004**, 4 (4), 587–590.
28. Majdoub, M. S.; Sharma, P.; Cagin, T. Enhanced Size-Dependent Piezoelectricity and Elasticity in Nanostructures Due to the Flexoelectric Effect. *Phys. Rev. Lett. B* **2008**, 77 (12), 125424-1–125424-9.

29. Bassiri-Gharb, N.; Fujii, I.; Hong, E.;Trolier-McKinstry, S.; Taylor, D. V.; Damjanovic, D. Domain Wall Contributions to the Properties of Piezoelectric Thin Films. *J. Electroceram.* **2007**, 19 (1), 47–67.

30. Wang, Y.; Ren, K.; Zhang, Q. M. Direct Piezoelectric Response of Piezopolymer Polyvinylidene Fluoride under High Mechanical Strain and Stress. *Appl. Phys. Lett.* **2007**, 91 (22), 222905-1–222905-3.

TOC Figure

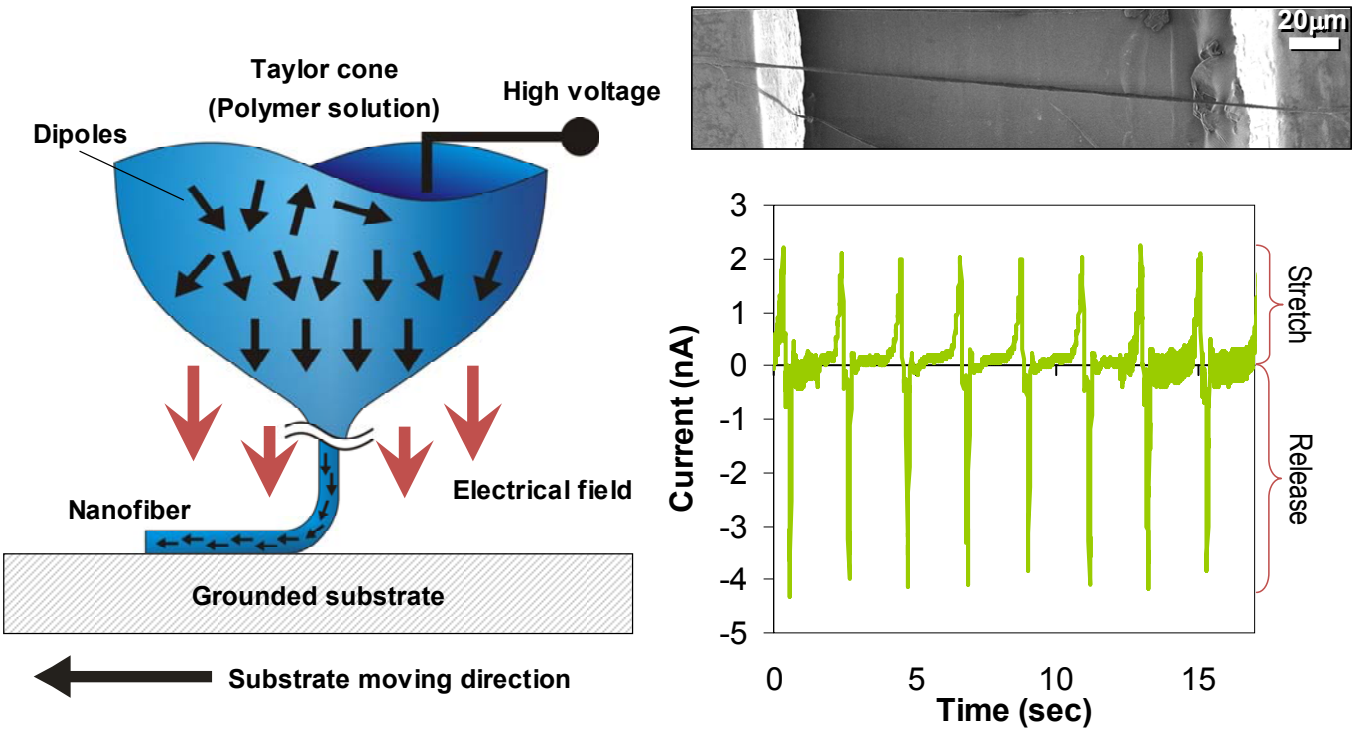

Supporting Information

MATERIALS AND METHODS

1. Polymer solution

The polymer solutions were made from polyvinylidene fluoride (PVDF) powders (*Mw* = 534 000) *(Sigma-Aldrich)*, N,N-Dimethylformamide (DMF) *(Sigma-Aldrich)*, acetone *(Sigma-Aldric)*, and Zonyl®UR *(DuPont)*. All reagents were not further purified or modified prior to generation of the solutions. Zonyl®UR is an anionic phosphate fluorosurfactant that was provided without solvents.

2. Poled PVDF thin film

Poled PVDF thin films *(Precision Acoustics*[S1]*)* were used for benchmark experimental testing. The films had dimensions of 5 cm × 5cm with thicknesses of 28 μm, 52 μm, and 110 μm with sputtered metal electrodes on the top and bottom surfaces. These films were cut into smaller pieces (4 – 8 mm wide and 9 – 15 mm long) and subsequently attached onto plastic substrates for experiments with glue.

3. Plastic substrate

The plastic testing substrates were made of TOPAS® 8007 Cyclic Olefin Copolymer via injection molding with a thickness of *c.* 0.75 mm, width of 25 – 30 mm, and length of 60 – 70 mm. 3M™ cleanroom high temperature ESD tape 1258 (0.07 mm thick) was applied on the top surface of the plastic substrate for enhanced electrostatic discharge performance. Finally, 3M™ aluminum conductive tape (0.05 mm thick) was cut and affixed to the tops of the ESD tape to serve as collectors for the NFES process and as electrodes for piezoelectricity measurements.

4. PVDF solution preparation

The PVDF solutions with DMF/acetone solvents were prepared using the following steps:

a. 1.8 g PVDF powder was dispersed in 4 g acetone for *c.* 30 minutes using a magnetic stirrer.
b. The complete PVDF solution was prepared by mixing 6 g DMF with the PVDF/acetone solution. 0.3 g Zonyl®UR was simultaneously added to the mixture. The mixture was then stirred for a minimum of one hour to reach sufficient homogeneity.
c. This surfactant caused intensive foaming during stirring, and the final was allowed to stand for another hour to rid the solution of foam.

All solutions were prepared and stored at room temperature in a well-ventilated laboratory environment. To minimize evaporation, all containers were sealed with Parafilm. Specific content of the solutions is listed in Table S1 below. The concentration of all substances is calculated in weight percentage (wt %) of the solvent.

Table S1. Experimental data of PVDF solution.

PVDF concentration	Solvent ratio (DMF : acetone)	Fluorosurfactant concentration
18 wt %	6 : 4	3 wt %

VALIDATION OF PIEZOELECTRIC RESPONSES

1. Non-piezoelectric polyethylene oxide nanofibers

To verify that the electrical outputs were generated from piezoelectric properties of PVDF nanofibers, we performed the same experiments but change the nanofiber material from PVDF to the non-piezoelectric polymer, poly(ethylene oxide) (PEO). The output voltage (Figure S1b) showed only noise with no visible peaks, indicating that PEO nanofibers did not produce piezoelectric behavior like the PVDF nanofiber (Fig. S1a). The data precluded the possibility of residual charges, friction, or contact potential as the cause of the observed electric outputs for the PVDF nanofibers.

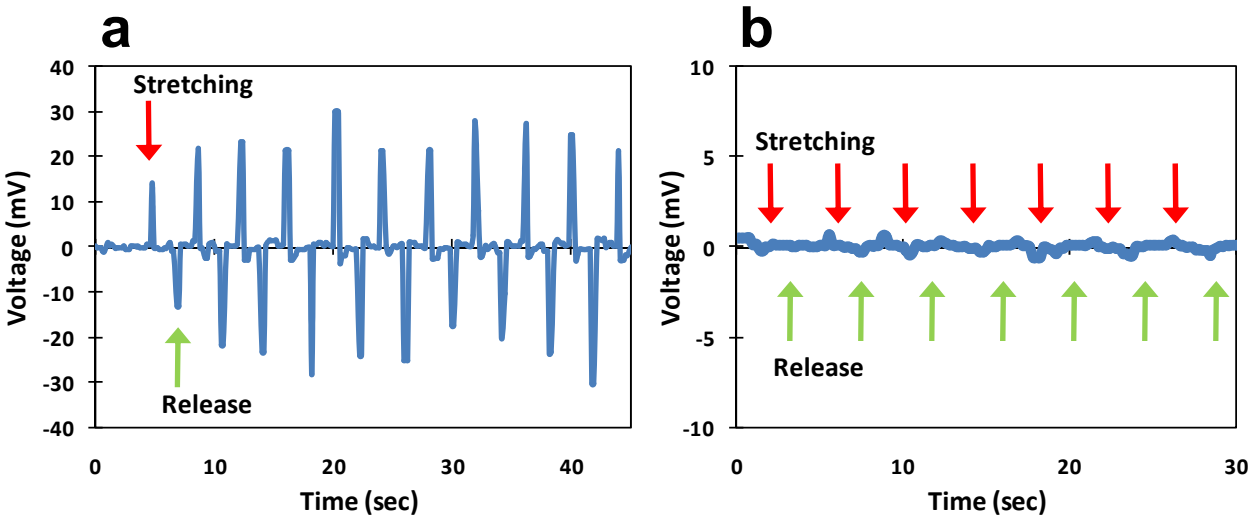

Figure S1. (a) Voltage output of a single PVDF nanofiber subject to continuous stretch and release. (b) Voltage output of a single PEO nanofiber subject to continuous stretch and release.

2. Randomly distributed PVDF nanofibers

By different electrode pattern design in conventional electrospinning, the electrostatic forces can guide PVDF nanofibers across the gap of two electrodes (Figure S2a). However, the PVDF nanofiber arrays do not have controlled polarity. The polarities of these PVDF nanofibers were still cancelling out one another such that the overall electric outputs were close to zero (Figure S2b).

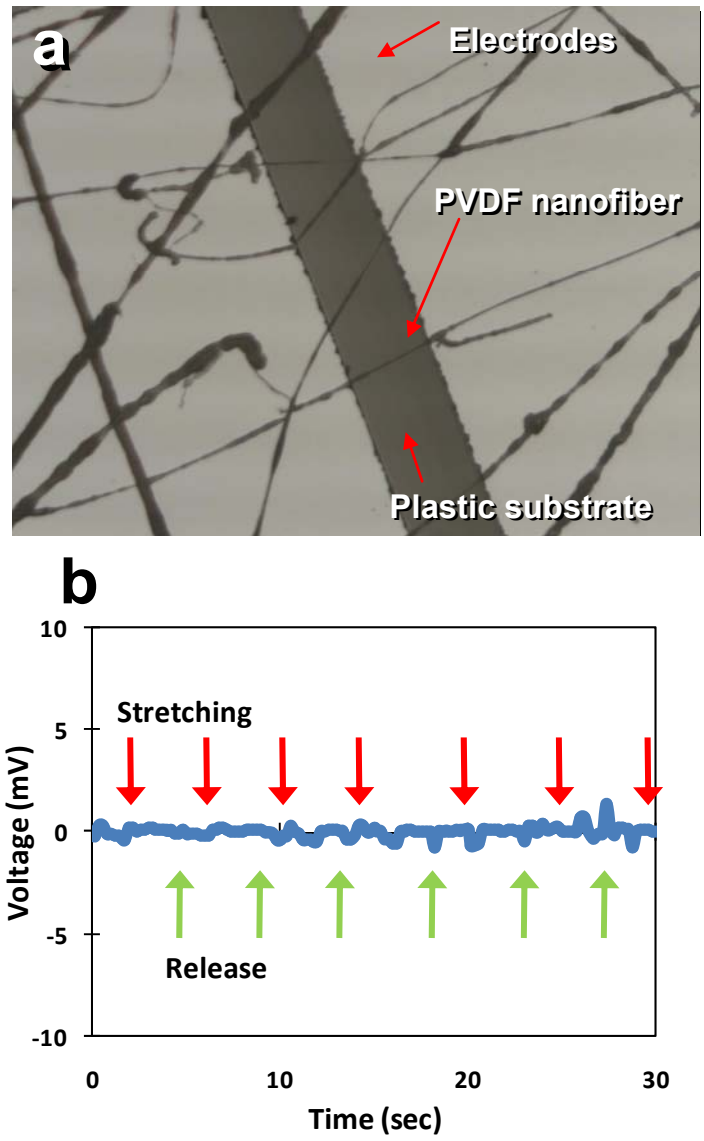

Figure S2. (a) Optical image of PVDF nanofibers deposited between two metal electrodes by conventional electrospinning. (b) Voltage output of the random PVDF nanofibers subject to continuous stretch and release.

3. Enhancement of electrical outputs

Enhanced outputs of voltage and current were demonstrated by making serial and parallel connections of nanogenerators as show in Fig. S3.

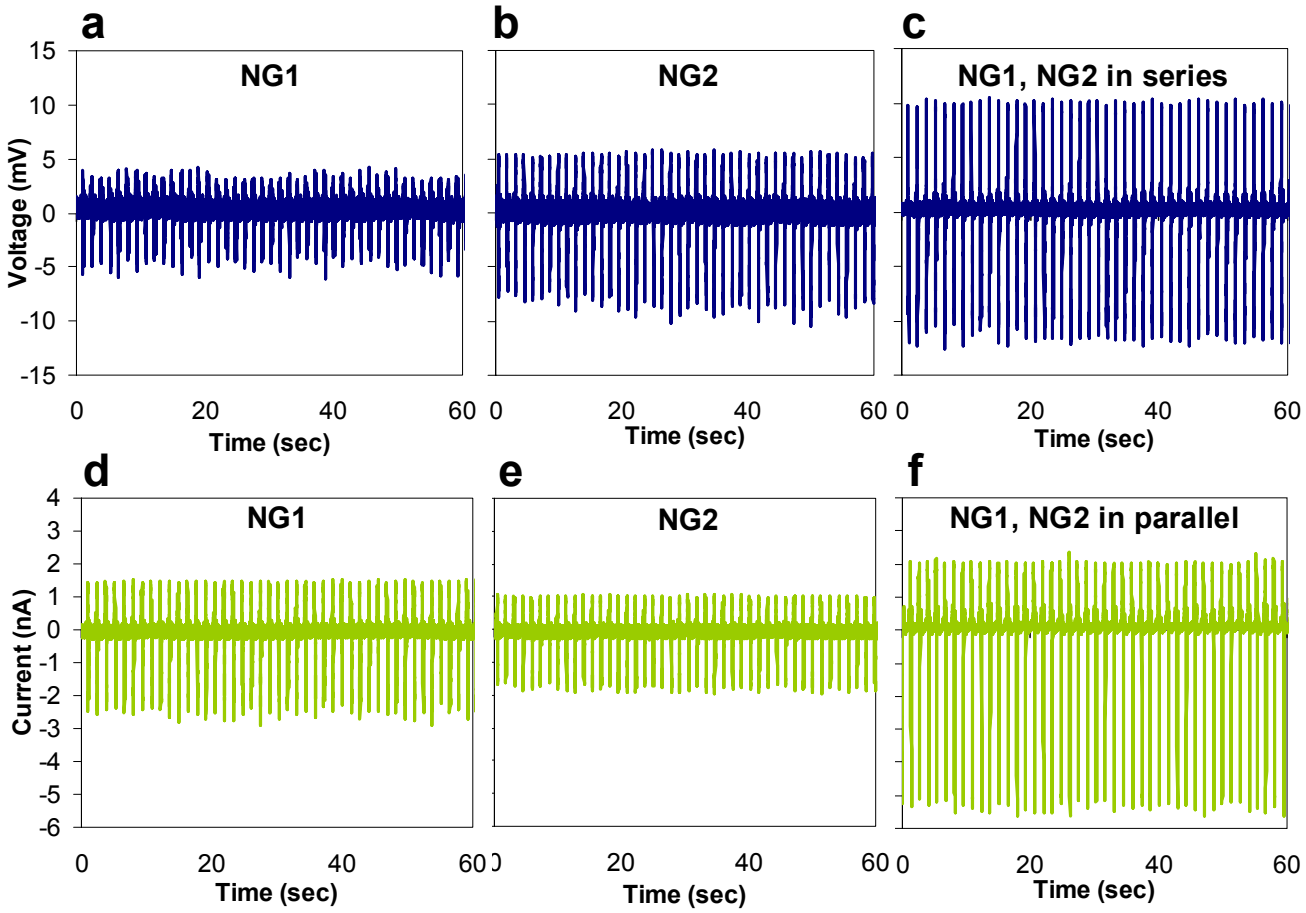

Figure S3. Output voltages of (a) nanogenerator #1 and (b) nanogenerator #2 subject to continuous stretch and release. (c) Output voltages constructively add when two nanogenerators are in serial connection. Output currents of (d) nanogenerator #1 and (e) nanogenerator #2 subject to continuous stretch and release. (f) Output currents constructively add when two nanogenerators are in parallel connection. All data are measured when the two nanogenerators are operated in the same strain, strain rate, and frequency.

ENERGY CONVERSION EFFICIENCY

The energy conversion efficiency (ECE) in this paper was defined as

$$\text{ECE} \equiv \frac{\textit{Electric energy generated}}{\textit{Mechanical energy applied}} = \kappa^2$$

where κ is the electromechanical coupling coefficient of the piezoelectric material. The electric energy W_e was estimated by integrating the product of output voltage and current of the PVDF nanogenerator when stretched. The elastic strain energy was estimated by using $W_s = \frac{1}{2} EA\varepsilon^2 L_0$, where E is Young's modulus of the material, A is cross-sectional area, ε is the strain applied on the material, and L_0 is the length of the material. The dimensions of the PVDF nanofibers were measured with SEM after the energy generation experiments. There were more than 45 PVDF nanogenerators used in our experiments to estimate the energy conversion efficiency. Among all samples in the energy conversion efficiency experiments, the nanofibers were 600 nm – 6.5 μm in diameter, 100 – 600 μm in length, and the Young's modulus was estimated as 1.4 GPa[S1].

The efficiency of the PVDF thin film was estimated using the same method as the PVDF nanogenerators. However, d_{31} mode was utilized in PVDF thin film instead of d_{33} mode to accommodate for the strain loading setup. In our experiments, the output voltage and current of the PVDF thin film were *c.* 60 mV and *c.* 60 μA, resulting in a energy conversion efficiency of 0.5 – 2.6% (average 1.3%). We realized that the energy conversion efficiency of d_{31} mode would be smaller than d_{33} mode (d_{33} = 30 pC/N and d_{31} = 22 pC/N from the company's data sheet[S1]). If taken into account, the efficiency would be enhanced by ~1.8 times, resulting in an average efficiency of 2.3%. However, it is noted that the real strain applied on the PVDF thin film would be larger than the strain on the top surface of the plastic substrate, which was measured by a strain gauge. Therefore, the energy conversion efficiency of the PVDF thin films would become smaller if we used the real strains on the PVDF thin films to calculate the efficiency. The energy conversion efficiency of PVDF thin film provided by the company was 1.96%, which was close to the estimate from our experiment. This demonstrated that the approach we used in calculating the energy conversion efficiency was reasonable.

The error analysis was performed to exam the repeatability and accuracy of our measurement system. First, we estimated the electrical energy error by calculating the average and standard deviation of electric energy generated from the same PVDF nanogenerator under the same operating conditions. As shown in Fig. S4 and Table S2, the calculated electric energy had an average of 4.07×10^{-13} J and a standard deviation of 8.74×10^{-14} J, corresponding to an error ($\Delta W_e / W_e$) of 21.5%. The elastic strain energy error mainly came from the mechanical strain variations, which was caused by the strain loading

S1. Vidhate, S.; Shaito, A.; Chung, J.; D'Souza, N. A. Crystallization, Mechanical, and Rheological Behavior of Polyvinylidene Fluoride-Carbon Nanofiber Composites. *J. Appl. Polym. Sci*. **2009**, 112, 254–260.

machine and plastic substrate. We estimated this error by continuously bending the plastic substrate by the same amount and measuring the strains to obtain the average and standard deviation. In our experiment, the measured strain had an average of 0.085% and a standard deviation of 0.0013%, corresponding to a strain error ($\Delta\varepsilon/\varepsilon$) of 1.5% and an elastic strain energy error ($\Delta W_s / W_s$) of 3.0%. Therefore, the total error of the energy conversion efficiency (ΔECE / ECE) was *c.* 21.71%.

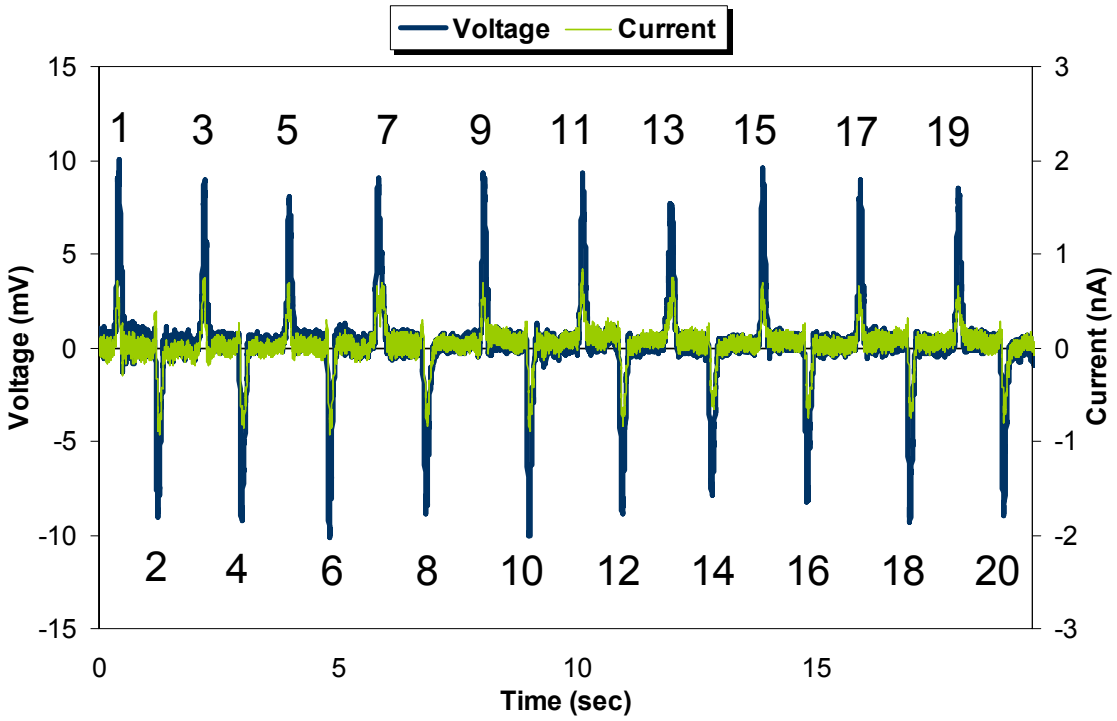

Figure S4. Output voltage and current of a PVDF nanogenerator subject to continuous stretch and release under the same strain.

Table S2. Calculated electric energy of PVDF nanogenerator.

No. of peaks	Electric energy (J)
1	3.23E-13
2	5.10E-13
3	3.28E-13
4	5.06E-13
5	3.03E-13
6	5.47E-13
7	4.76E-13
8	4.56E-13
9	3.09E-13
10	5.38E-13
11	3.93E-13
12	4.83E-13
13	4.06E-13
14	3.86E-13
15	3.03E-13
16	4.21E-13
17	2.64E-13
18	4.51E-13
19	2.89E-13
20	4.39E-13
Average	**4.07E-13**
Standard deviation	**8.74E-14**